

PRZEMYSŁAW SKOTNICZNY\*<sup>#</sup>, PIOTR OSTROGÓRSKI\*<sup>#</sup>**THREE-DIMENSIONAL AIR VELOCITY DISTRIBUTIONS IN THE VICINITY  
OF A MINE HEADING'S SIDEWALL****TRÓJWYMIAROWE ROZKŁADY WEKTORA PRĘDKOŚCI POWIETRZA  
W STREFIE PRZYOCIOSOWEJ WYROBISKA GÓRNICZEGO**

The presented paper describes the results of an experiment determining the instantaneous values of velocity vector components of the air stream at selected spots of the boundary layer formed at the sidewalls of the mine heading in the ŁP type steel arch support. The experiment was carried out in a mine heading in an active hard coal mine. A 3-axis thermoanemometric probe was used to obtain three-dimensional distributions of the velocity and turbulent values, such as turbulence intensity and turbulent kinetic energy of the flowing ventilation air stream. The analysis of the measurement results was aided by a numerical solution of the discussed case of flow.

The research results presented in this paper provide a basis for extensive studies of the description of velocity distribution and other turbulent quantities within the near-sidewall structures of a mine heading. The objective of these tasks is to improve the accuracy and reliability of numerical calculations relating to air flow in mine headings.

**Keywords:** 3-axis thermoanemometric probe, velocity profile measurement in mine heading, numerical solution validation

W artykule opisano wyniki eksperymentu polegającego na wyznaczeniu chwilowych wartości składowych wektora prędkości strugi powietrza w wybranych punktach warstwy przyściennej tworzącej się przy ociosach wyrobiska górniczego prowadzonego w obudowie typu ŁP. Eksperyment przeprowadzono w wyrobisku górniczym w czynnej kopalni węgla kamiennego. Przy pomocy trójwłókowej sondy termomanometrycznej uzyskano trójwymiarowe rozkłady prędkości oraz rozkłady wielkości turbulentnych takich jak intensywność turbulencji i energia kinetyczna turbulencji przepływającej strugi powietrza wentylacyjnego. Analiza wyników pomiarów została wzbogacona rozwiązaniem numerycznym omawianego przypadku przepływowego.

Przedstawione w artykule wyniki badań stanowią podstawę rozbudowanych studiów nad opisem rozkładu prędkości oraz pozostałych wielkości turbulentnych w obrębie struktur przyociosowych wyro-

\* STRATA MECHANICS RESEARCH INSTITUTE OF THE POLISH ACADEMY OF SCIENCES, UL. REYMONTA 27, 30-059 KRAKOW, POLAND

# Corresponding author: [skotnicz@img-pan.krakow.pl](mailto:skotnicz@img-pan.krakow.pl); [ostrogorski@img-pan.krakow.pl](mailto:ostrogorski@img-pan.krakow.pl)

biska górniczego. Celem podjętych prac jest poprawa dokładności i rzetelności obliczeń numerycznych przepływu powietrza w wyrobiskach górniczych.

**Słowa kluczowe:** sonda termooanemometryczna trójwłóknowa, pomiar profilu prędkości w wyrobisku górniczym, walidacja rozwiązania numerycznego

## 1. Introduction

The distribution of the velocity vector of the air stream and its turbulent parameters in the vicinity of mine headings plays a key role not only in the proper determination of an average velocity in the selected heading cross-section, but also during the process of numerical solution validation.

A correctly estimated value of the average velocity vector is necessary to determine the volumetric stream of the air flowing in the pre-defined heading cross-section and, in turn, the distribution of the velocity vector of the flowing air stream, and determined turbulent quantities at individual spots facilitate the decision on the location of a stationary anemometer in the cross-section of the heading. The knowledge about the quantities in question also facilitates designing and performing a proper numerical simulation of the air stream transport process in the mine heading, which is particularly important for the case of the air and methane mixture flow.

In the network of mine headings, stationary vane anemometers are conventionally located at selected spots; the devices are part of the telemetric network in the mine. Their main function is to measure air velocity in crucial regions of the ventilation network. Due to their mode of operation, they cannot serve as a source of experimental data required to determine fast-changing distributions of the velocity vector. Hence, it was necessary to apply an instrument suitable for measurements at selected spots of the heading cross-section and with an option to record fast-changing functions of velocity components of the flowing ventilation air stream.

This criterion was met by the thermoanemometric system based on 3-axis sensors; the system was used to determine spatial parameters of the structure forming in the vicinity of the mine heading's side wall in the LP type steel arch support.

## 2. Experiment in the mine

The measurements were taken at the TW Sobieski hard coal mine, at level 500, in the cutting referred to as Grodzisko (Skotniczny, 2015), in two selected measurement cross-sections. The layout of the measuring stations is shown in the following map (Fig. 1).

In the selected measurement cross-sections, components of the velocity vector in the vicinity of heading sidewalls were measured.

The measurements were taken with a multi-channel thermoanemometric system (Skotniczny, 2015) adapted to mine conditions and suitable for determining components of the velocity vector in the directions  $U_1$ ,  $U_2$ ,  $U_3$  and the corresponding intensity of transverse ( $T_{U2}$ ,  $T_{U3}$ ) and longitudinal ( $T_{U1}$ ) turbulences.

The headings in both measurement cross-sections were arranged in the LP type steel arch support. In the heading where measurement Cross-section 1 was located, the spacing of the support frame was approximately 0.8 m, whereas in the heading with Cross-section 2 – approximately

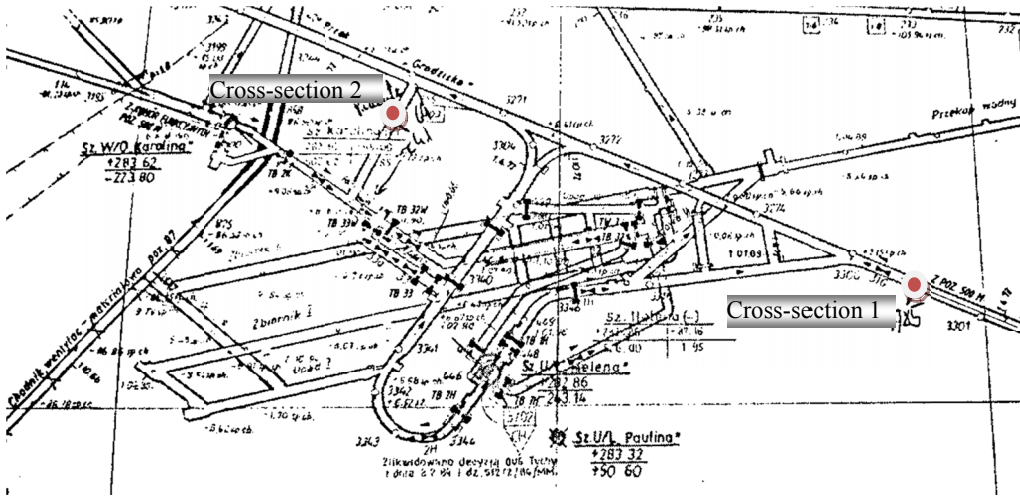


Fig. 1. Section of the 300-level map with marked measurement spots

0.5 m. Dimensions of individual headings in the locations of the measurement cross-sections were as follows:

- Cross-section 1: L = 4.8 m;  
H = 3.2 m.
- Cross-section 2: L = 3.4 m;  
H = 3.4 m.

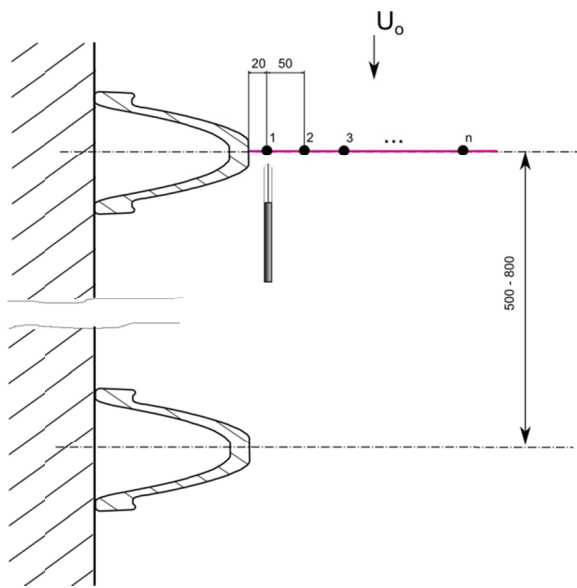


Fig. 2. Measurement cross-section.  $U_0$  – free stream velocity

A schematic view of the measurements is presented in Fig. 2. The 3-axis sensor was routed along a straight line, perpendicular to the arch of the support frame. The first measurement spot was located at an approximate distance of 20 mm from the arch. Other spots were spaced at 50 mm from each other. During the measurements, up to 25 measurement spots were recording in a single series.

In Cross-section 1, two measurements were completed along one probing line parallel to the floor, whereas five measurements were taken along the same probing line in Cross-section 2.

The thermoanemometric probe was mounted using an extension arm held by the grip of the stand. The distance between subsequent measurement spots was modified by moving the extension arm together with the probe by the required distance.

During the measurements, a total of 200 records were saved in files with measurement data.

### 3. Instrumentation and measurement method

The measurements were taken with a 3-axis thermoanemometric system (Fig. 3b), whose suitability was verified during underground measurements (Krawczyk et al., 2011). The data was obtained by measurements taken with a single 3-axis thermoanemometric probe (Fig. 3b). Using a single probe facilitated obtaining a higher spatial resolution of the measurements without the need for time-consuming conversion of spatial coordinates as would be the case for a full set of probes.



Fig. 3. Multi-channel thermoanemometric system a) with a thermoanemometric probe b)

A single measurement series at the selected spot of the heading cross-section provided the time vector consisting of  $4 \times 4096$  records. The vector was saved in a text file to be then processed statistically.

It was necessary to transform the coordinate system due to the fact that the 3-axis probe was designed to measure the velocity vector of the flowing air in the coordinate system associated with the probe axis (marked in Fig. 4 as X1, Y1, Z1), and the discussed measurements required measurements of the vector in the coordinate system associated with the heading axis (X2, Y2, Z2). The most effective method was to apply a transformation consisting in three rotations around the axes of the reference system. This method is known as *Euler angles* (Bronsztejn & Siemiendajew, 2010). This is a system of three angles that allow unambiguous determination of mutual orientation of two Cartesian coordinate systems of the same helicity in the three-dimensional Euclidean space.

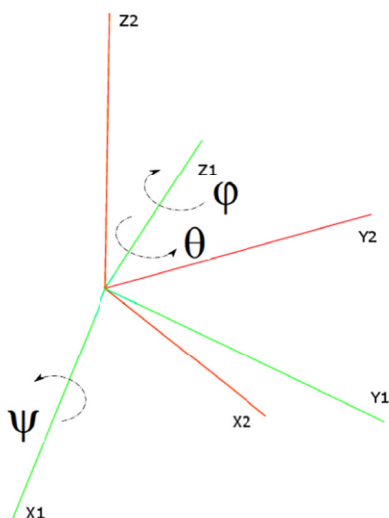


Fig. 4. Change of the coordinate system

The required transformation was obtained for the angles  $\varphi = -45^\circ$ ,  $\psi = 35.4^\circ$  and  $\theta = 90^\circ$ . The matrix of the total rotation of the system X1, Y1, Z1 to obtain the system X2, Y2, Z2 is as follows:

$$\begin{pmatrix} \cos(\psi) \cdot \cos(\varphi) - \sin(\psi) \cdot \cos(\theta) \cdot \sin(\varphi) & \cos(\psi) \cdot \sin(\varphi) - \sin(\psi) \cdot \cos(\theta) \cdot \cos(\varphi) & \sin(\psi) \cdot \sin(\theta) \\ \sin(\psi) \cdot \cos(\varphi) + \cos(\psi) \cdot \cos(\theta) \cdot \sin(\varphi) & -\sin(\psi) \cdot \sin(\varphi) + \cos(\psi) \cdot \cos(\theta) \cdot \cos(\varphi) & -\cos(\psi) \cdot \sin(\theta) \\ \sin(\theta) \cdot \sin(\varphi) & \sin(\theta) \cdot \cos(\varphi) & \cos(\theta) \end{pmatrix}$$

The value of the elements in the above matrix for the known rotation angles is:

$$\begin{bmatrix} 0.5764 & 0.4096 & -0.7071 \\ 0.5764 & 0.4096 & 0.7071 \\ 0.5793 & -0.8151 & 0 \end{bmatrix}$$

Following appropriate calculations, the set of velocity vectors obtained in a single measurement series was presented in a new coordinate system (Skotniczny, 2015).

After the transformation, the experimental data was further processed using the dedicated “R4” software that made it possible to calculate values of average velocities  $U_1, U_2, U_3$ , turbulence intensity  $T$  and turbulent kinetic energy  $E_k$  in subsequent measurement spots. Individual quantities were determined using the following expressions:

- average values of velocity vector components at  $U_i$

$$U_i = E[u_i(t)] = \frac{1}{T} \int_t^{t+T} u_i(x_0, t) dt \quad \text{for } i = 1, 2, 3 \quad (1)$$

which, for probability distribution  $u$  close to normal distribution, assumes the value of the arithmetic mean of the time function  $u_i(t)$ , the average velocity at the spot was determined using the relationship:

$$|U| = \sqrt{U_1^2 + U_2^2 + U_3^2} \quad (2)$$

- transverse turbulence intensity for  $i = 2, 3$  and longitudinal turbulence intensity for  $i = 1$

$$T_{u_i} = \frac{1}{U_0} \sqrt{u_i^2} \quad (3)$$

where  $\sqrt{u_i^2}$  — standard deviation  $u_i$

- turbulence intensity

$$T = \sqrt{\frac{1}{3}(T_{u1}^2 + T_{u2}^2 + T_{u3}^2)} \quad (4)$$

- and values of diagonal components of the Reynolds stress tensor

$$\overline{u_i^2} = \overline{u_i u_i} = \sum_{k=0}^N (u_{ik} - \overline{U_i})(u_{ik} - \overline{U_i}) \quad (5)$$

- to be later used to calculate the value of turbulent kinetic energy in accordance with the following formula:

$$E_k = \frac{1}{2} (\overline{u_1^2} + \overline{u_2^2} + \overline{u_3^2}) \quad (6)$$

The results of calculations are plotted below for the measurement cross-sections: “Cross-section 1” and “Cross-section 2”.

## 4. Measurement results

### Cross-section 1.

The change of values of velocity vector components at individual measurement spots in the function of the distance from the sidewall for the measurements A, B recorded along the probing line in Cross-section 1 are shown in Fig. 5.

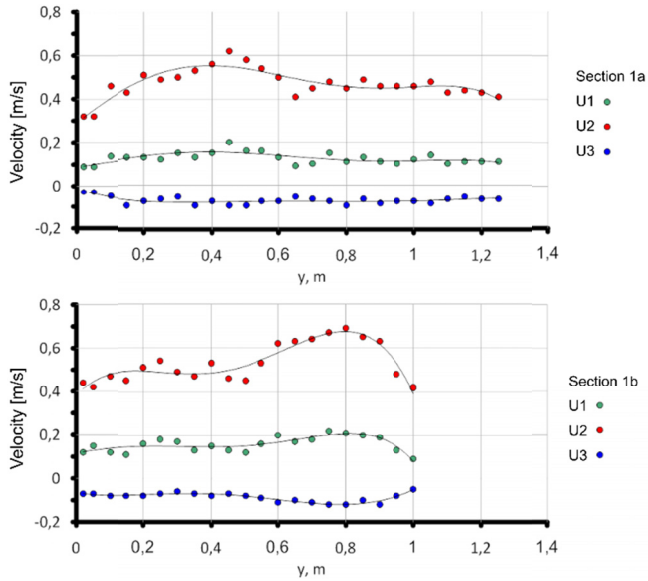


Fig. 5. Change of values of velocity vector components at individual measurement spots in the function of distance from the sidewall – “Cross-section 1”

Fig. 6 shows changes of values of turbulence intensity  $T$  and turbulent kinetic energy  $Ek$  at individual measurement spots in the function of distance from the sidewall.

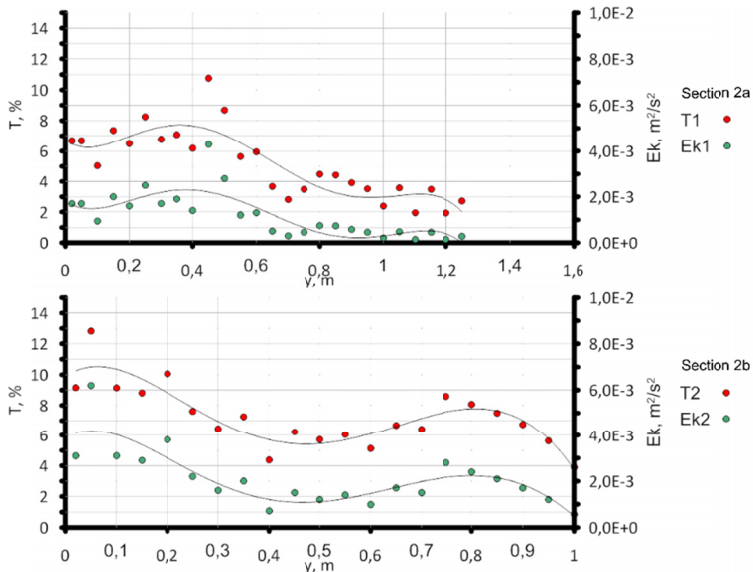


Fig. 6. Change of values of turbulence intensity  $T$  and turbulent kinetic energy  $Ek$  at individual measurement spots in the function of distance from the sidewall – “Cross-section 1”

The irregular variation of components  $U_1$ ,  $U_2$ ,  $U_3$  was first caused by a highly non-stationary flow of the air stream in the measurement “Cross-section 1”. The following figure (Fig. 7) presents the change of the average velocity along the heading axis, as measured with the mAS4 anemometer.

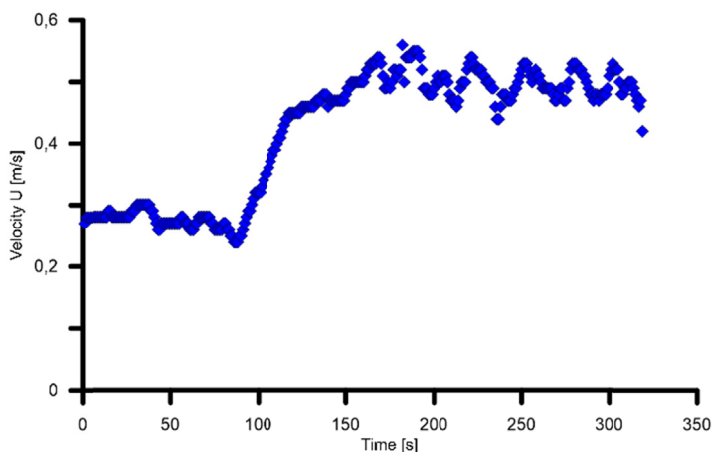


Fig. 7. Recorded changes of the average velocity in the axis of the Grodzisko heading (Cross-section 1) in the function of time

It easily noticeable that the average velocity of the ventilation air flowing through the Grodzisko cutting increased from approximately 0.3 m/s to approximately 0.5 m/s during a part of the measurement taken with the thermoanemometric system. In addition, the change of the velocity value was accompanied by long-lasting average velocity fluctuation (observable from the time  $t = 150$  s), associated most probably with a step change of pressure due to the opening of the ventilation brattice.

Another factor affecting the low reliability of the measurement data obtained for Cross-section 1 are very low values of the average velocity of the air flowing through the cutting. It is assumed that thermoanemometric probes can be used at a velocity below 0.5 to 0.6 m/s provided that the probes undergo special calibration procedures when such conditions are anticipated. Velocities ranging from 0.2 to 0.5 m/s are very close to convective velocities, and thus the velocity measured with a thermoanemometer under such conditions is a superposition of the advective and convective movements caused by a heated wire.

This phenomenon may be confirmed to some extent by the variation of turbulent intensity and turbulent kinetic energy, as shown in Fig. 6. For flow velocities of 0.5 m/s, the anticipated value of turbulence intensity in the heading axis should not exceed 2% to 3% and, in the observed flow, particularly the second measurement (section 1b), the intensity value varies from 4% to 8%. Elevated T values may suggest a major influence of convection on the process of energy exchange between the heated wire and the surroundings.

For this reason, it was decided to continue the measurements in Cross-section 2, where the average measured velocity in the heading axis was 2.8 to 3.4 m/s and the variation of the flow value over time was as presented in the graph in Fig. 8.

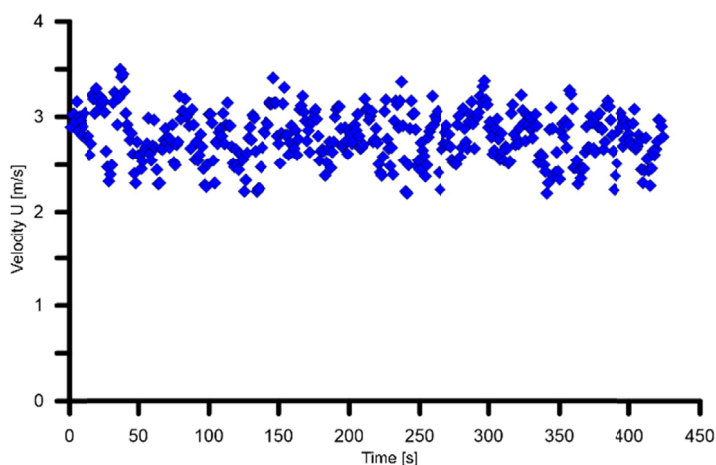


Fig. 8. Recorded changes of the average velocity in the heading axis in the function of time – “Cross-section 2”

### **Cross-section 2.**

The graphs in Fig. 9 show changes of values of velocity vector components relating to the flowing air stream in the function of distance from the sidewall for “Cross-section 2” during measurements a, b, c, d and e, as recorded along the probing line.

Unlike the changes recorded in “Cross-section 1”, it is noticeable for the curves in Fig. 9 that there is a distinct monotonous distribution of the component  $U_1$  (dominant component in the flow – parallel to the heading axis), indicating the presence of a stable layer in the vicinity of the wall for the measurement cross-section being discussed. The perpendicular components ( $U_2, U_3$ ) demonstrate almost uniform distribution in the function of distance from the sidewall, meaning that the flow has a highly anisotropic nature. However, the occurrence of non-zero values of components  $U_2, U_3$  caused a slight deviation of velocity vector  $U_d$  in the direction parallel to the heading axis. This phenomenon may be observed in Fig. 10.

While analysing spatial distributions of average velocity vectors recorded at the measurement spots in Cross-section 2 (Fig. 10), one may observe that the deviation of vector directions on the plane  $U_1U_3$  might be caused by the presence of arches of the support frame. However, deviations of vectors might be additionally caused by a non-uniform velocity field in the heading cross-section due to the already observed movements of brattices (Cross-section 1). This phenomenon can also occur in Cross-section 2; it is less prominent due to the “filtering” effect of heading volume of the bottom of the Karolina shaft.

Some evidence of this circumstance can be sought by analysing value changes of turbulence intensity and turbulent kinetic energy – as shown in Fig. 11.

Both  $T$  and  $Ek$  values decrease in the direction of the heading axis, indicating the transition from the sidewall layer zone towards the direction of the region occupied by the potential core. However, this change is not continuous, which suggests slight changes of flow conditions during the measurement. This is especially well visible in Fig. 11 for Cross-sections 2c and 2e.

At a distance of approximately 0.85 to 1 m from the sidewall, there is a step increase of both  $T$  and  $Ek$ , which may directly suggest an instantaneous change of the flow velocity. This

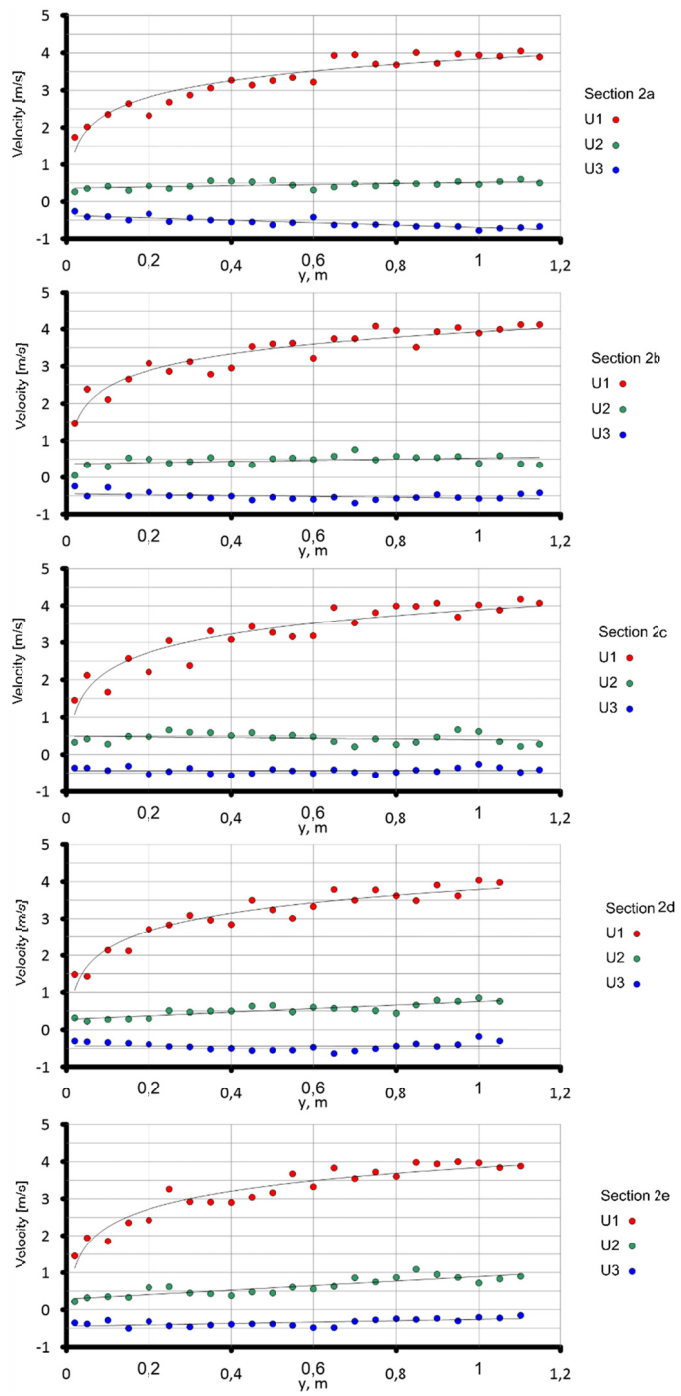


Fig. 9. Change of values of velocity vector components at individual measurement spots in the function of distance from the sidewall – “Cross-section 2”

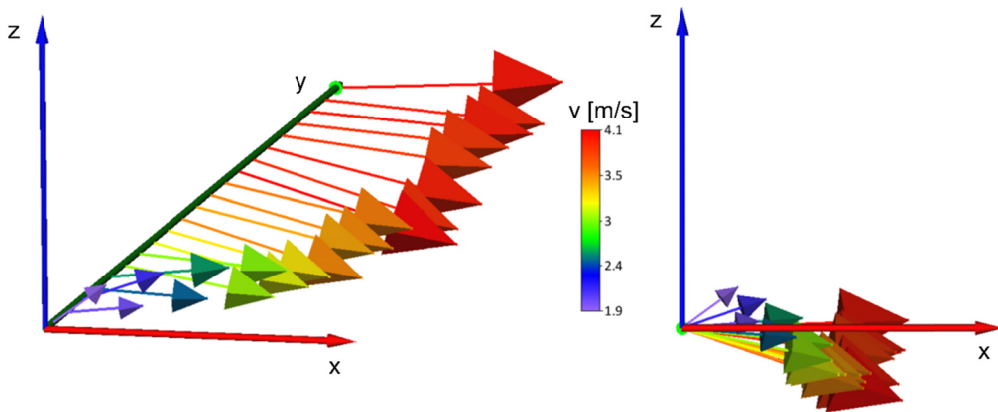


Fig. 10. Spatial distribution of the velocity vector in “Cross-section 2”

phenomenon is less visible for velocity profiles (Fig. 10) due to the applied procedure for averaging the measured velocity values.

## 5. Numerical analysis of the case

The analysis presented in the previous chapter indicated the potential coexistence of two phenomena that may affect the distribution of the velocity vector of the air stream flowing in the vicinity of the sidewall of the mine heading:

1. Non-stationary nature of average flow;
2. Presence of arches of the LP type support.

In order to verify such observations, it was necessary to apply numerical analysis to the case in question. Therefore, a computational domain was designed (a section of the heading with arch type support frame). Next, calculations were completed with the known experimental measurements of values of the boundary conditions:

- velocity of the air stream at the inlet of the heading  $|U| = 3.9$  m/s;
- turbulence intensity  $T = 10\%$ ;
- mixing path  $l_m = 0.273$ .

The calculations were completed using the *SAS* model (*Scaled Adaptive Simulation*) (Fluent User Manual, 2004; Menter, F.R., et al. 2003; Menter, F.R., Egorov Y., 2005) in the ANSYS Fluent software, assuming a non-stationary isothermal turbulent flow with a time step of  $\Delta t = 1e^{-3}$  s. Additionally, the calculations involved a spectral perturbation synthesiser (Fluent User Manual, 2004) at the inlet of the computational domain. This measure supplemented the value of the average air flow velocity at the inlet with additional whirl structures (perturbations) introduced in the form of a frequency spectrum.

For simplification, the analysis was carried out for the two-dimensional case, and the computational domain was established on the measurement cross-section plane parallel to the floor of the heading (Fig. 12 – rectangular area).

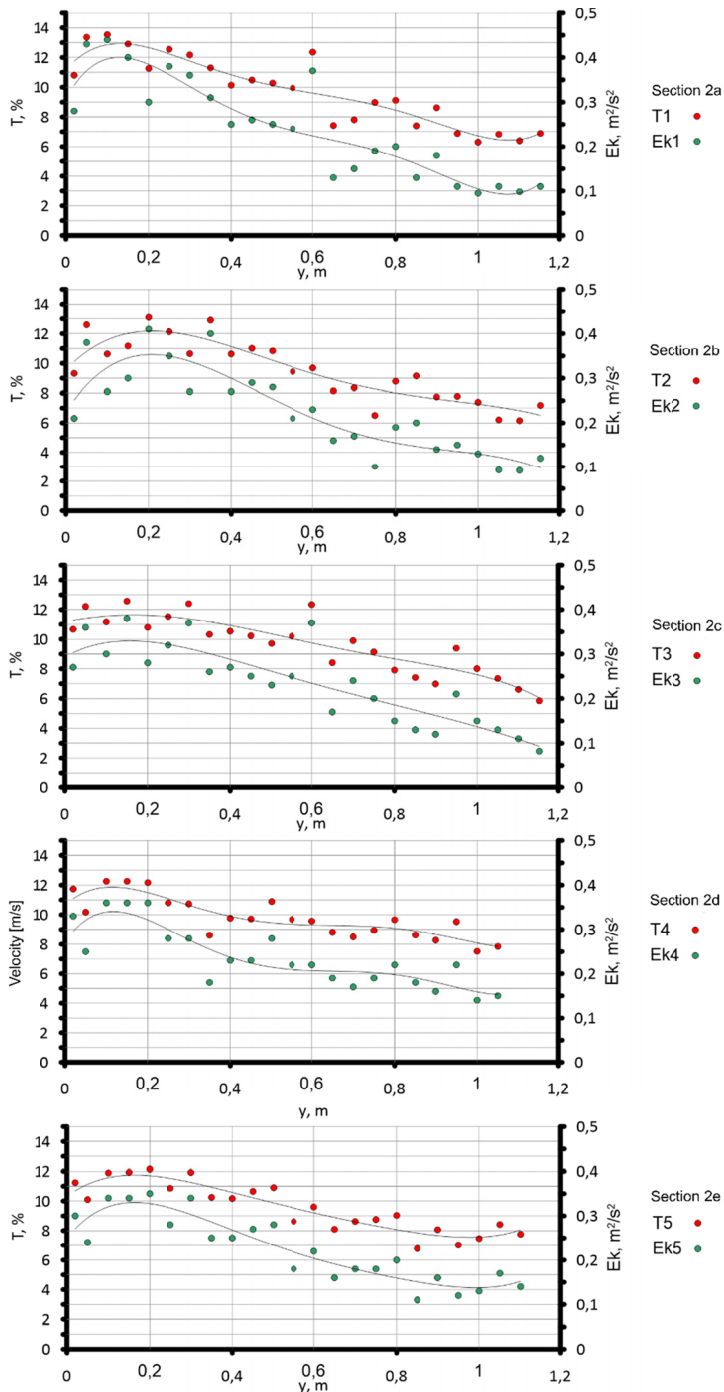


Fig. 11. Change of values of turbulence intensity  $T$  and turbulent kinetic energy  $Ek$  at individual measurement spots in the function of distance from the sidewall – “Cross-section 2”

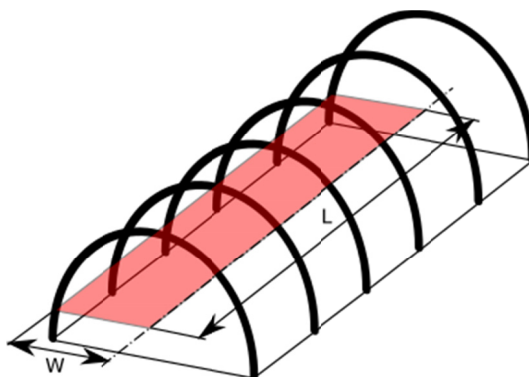


Fig. 12. Diagram of how the two-dimensional computational domain was established

The two-dimensional computational region had a width of  $W = 1.7$  m (from the sidewall to the headline axis) and a span of  $L = 20$  m. Within this region, there were 40 arches of the LP support. Due to the shape of the arches, the applied calculation grid was a Tri-Pave non-structural one, with a total number of elements amounting to 225,000. A section of the calculation grid is shown in Fig. 13.

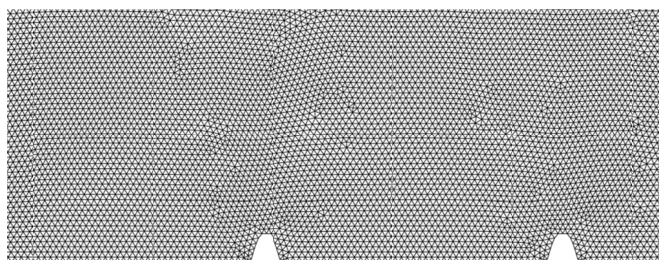


Fig. 13. Section of the calculation grid

The function of the calculated velocity profile  $|U|$  for a selected time instant, compared with the experiment results, is presented in Fig. 14.

The variation functions of turbulence intensity  $T$  and turbulent kinetic energy, compared with experiment values, are presented in Fig. 15 and Fig. 16, respectively.

While analysing the functions in Fig. 14, 15 and 16, it is noticeable that the experimental functions differ from those obtained by means of numerical calculations. The differences between the measured and calculated values are particularly demonstrated by the graphs presenting the function of turbulence intensity and turbulent kinetic energy changes. Most likely, the observed difference is caused by the non-stationary nature of the air flow in the computational domain, being intensified by the presence of arches of the support frame. As a result, the obtained values of distribution within the sidewall zone may be a superposition of several or more various profiles.

The easiest method to illustrate the phenomenon is to use a colourful turbulence intensity  $T$  map for selected time instants (Fig. 17).

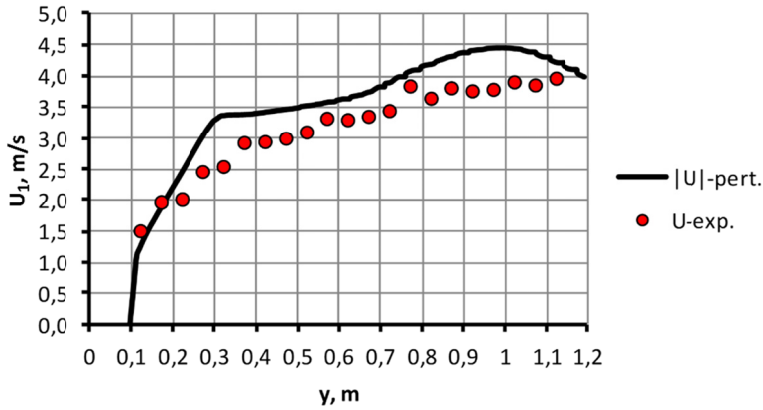


Fig. 14.  $|U|$  velocity in the function of distance from the sidewall  $y$ . Solid line – numerical calculations, dots – experiment

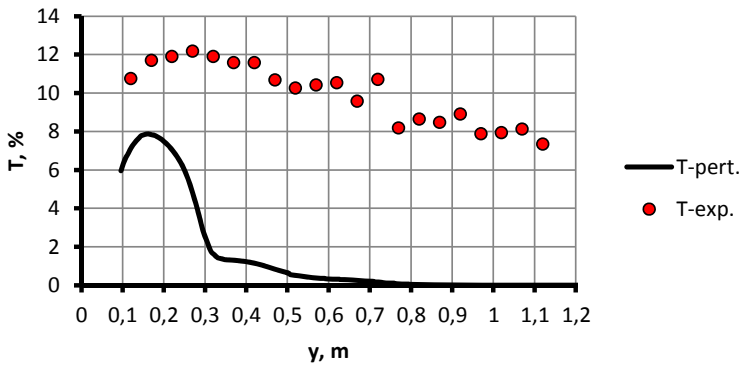


Fig. 15.  $T$  variation in the function of distance from the sidewall  $y$ . Solid line – numerical calculations, dots – experiment

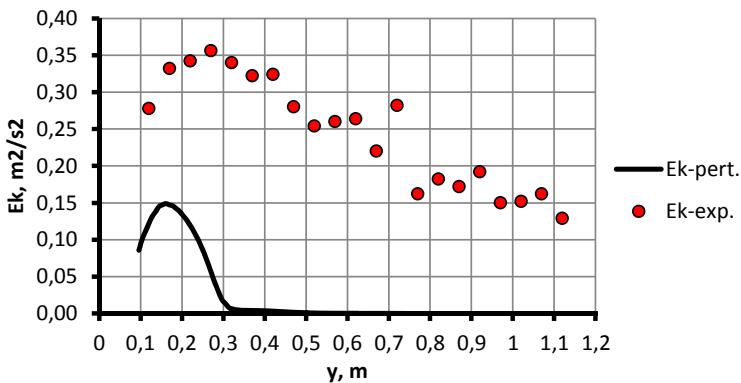


Fig. 16.  $E_k$  variation in the function of distance from the sidewall  $y$ . Solid line – numerical calculations, dots – experiment

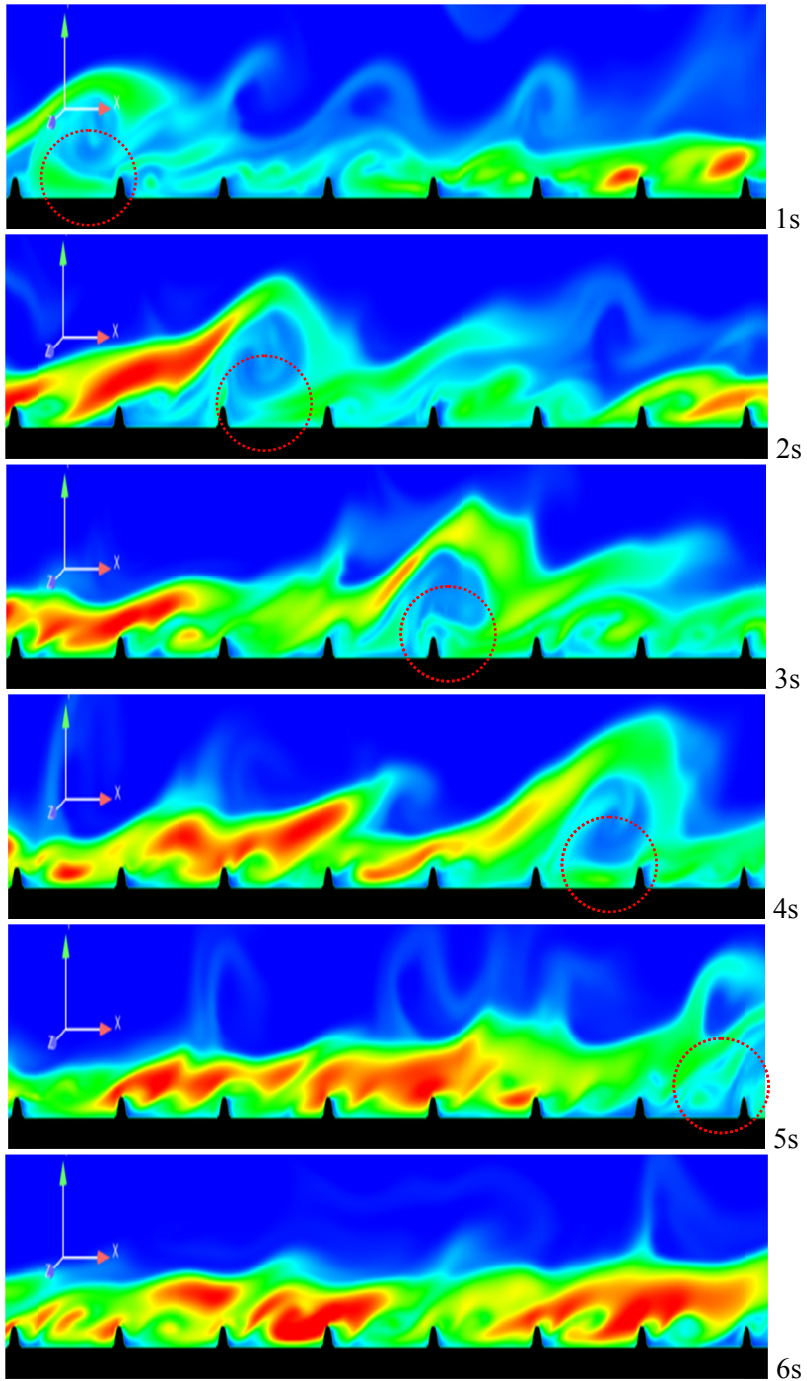


Fig. 17. Isosurfaces of turbulence intensity  $T$ . Calculations with a spectral synthesiser at the inlet of the computational domain

Fig. 17 shows isosurfaces of turbulence intensity for six of the selected time steps. The time shift for all presented isosurfaces was  $\Delta t = 1$  s.

In the figures, the circle marks the region with the beginning of formation of the whirl structure in the vicinity of the sidewall and its propagation during subsequent simulation instants. The cohesion of the whirl structure in advective transport was possible due to the constant effect of the turbulence generated at subsequent arches of the support frame. However, the process was not continuous because no formation of a new structure in the same place accompanied the structure displacement outside the region in question. This phenomenon may indicate the occurrence of intermittency in the flow of the air stream in the mine heading.

In contrast to the above-mentioned results, the flow analysis with a conventional SAS model generate data that remain constant with time, once the flow becomes steady. This is illustrated in Fig. 18:

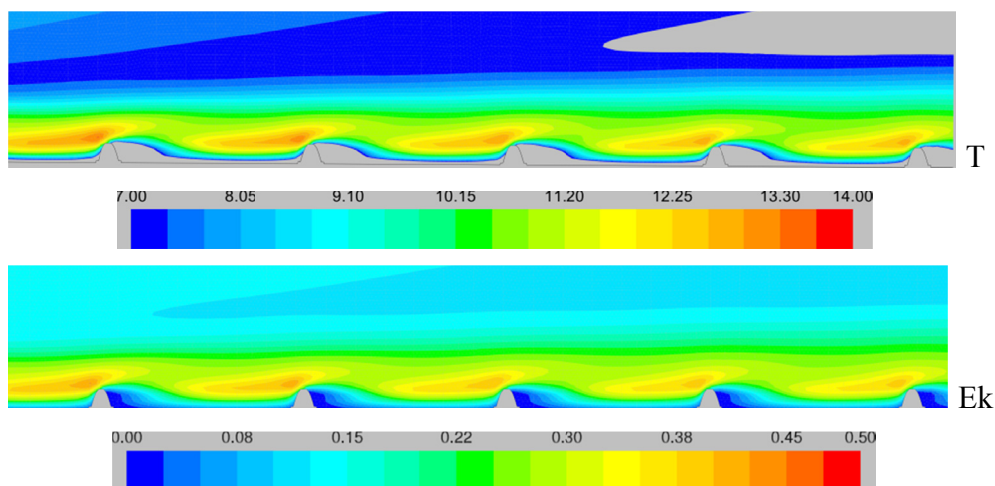


Fig. 18. Isosurfaces of turbulence intensity  $T$ . Calculations without perturbations at the inlet of the computational domain

Once the flow becomes steady (in the discussed case, the time was 5 s), the isosurfaces of turbulence intensity and turbulent kinetic energy remained unchanged, independently of the time of simulation. In this case, the only “turbulence mixer” of the air stream flow was created by the arches of the LP support, the presence of which caused an increase in turbulence intensity by 14% and turbulent kinetic energy  $Ek = 0.52 \text{ m}^2/\text{s}^2$ . Unfortunately, a simpler solution, i.e. a solution without the non-stationary factor, did not correspond to the actual image of air flow in the mine heading.

## 6. Summary and conclusions

This paper presented the results of experimental research on three-dimensional turbulent structures formed during air flow in the vicinity of sidewalls of the mine heading arranged in

the LP type steel arch support. The measurements involved a multi-channel thermoanemometric system suitable for measuring components of the velocity vector at selected spots of the measuring cross-section. The measurements were taken in actual conditions, during normal operation of the mine. In the two available measurement cross-sections, all measurements were taken only in Cross-section 2. For Cross-section 1, the reason was the insufficiently high value of the average flow velocity (below 0.6 m/s) and the occurrence of high non-stationary aspects in the flow was caused due to the movement of brattices.

The analysis of the measurement data concluded that, in the preliminarily accepted flow aspect of the measurement Cross-section 2, it is possible to notice traces of non-stationary air stream flow caused most probably by the already mentioned movement of brattices. Specific flow conditions in the shaft bottom region of the Karolina shaft only slightly improved the quality of air stream by means of flow homogenisation.

Due to the likely occurrence of non-stationary flows, indicating intermittency, it will be necessary in the future to extend the time of a single measurement to approximately 20 s (as estimated), at the sampling rate at least 1 kHz. In conjunction with a high probability of occurrence of non-stationary flows, it is also necessary to introduce a simultaneous multi-point measurement of turbulent structures forming in the air flow in the mine heading. This measurement method will be suitable to provide unambiguous recording of velocity profiles and turbulent quantities of the air stream at the required time instant.

The application of 3-axis thermoanemometers in headings certainly introduces an additional cognitive value and, eventually, will aid the development of numerical methods to be deployed for calculations of complicated flow cases occurring in underground headings. Obviously, one must remember that thermoanemometric probes can be used for research only under controlled conditions due to their durability.

The presented numerical solution for the model of the air flow in the vicinity of a sidewall made it possible to understand the mass transport mechanism in the mine heading, which will have a positive influence on the design of following measurement experiments. However, please note that the presented numerical solution must not be deemed complete. In order to obtain the whole image of fluid flow in the mine heading, it is necessary to design a three-dimensional computational domain, together with a corresponding grid, and then adjust the model based on an expanded measurement experiment.

## Acknowledgments

This publication is a presentation of the results obtained during the performance of Subtask 2.1: *Preparation and performance of laboratory and in situ experiments* under the statutory activities of the Strata Mechanics Research Institute of the Polish Academy of Science in 2017.

## References

- ANSYS Inc., *Fluent User Manual*. 2004.
- Bronsztejn I.N., Siemiendajew K.A., 2010. *Matematyka: poradnik encyklopedyczny*. Warszawa.
- Menter F.R., Egorov Y., 2005. *A scale adaptive simulation model using two equations models*. 43 AIAA Aerospace Sciences Meeting and Exhibit, Reno, Nevada, 10-13 January 2005.

- Menter F.R., Kuntz M., Bender R., 2003. *A scale-adaptive simulation model for turbulent flow predictions*. AIAA Paper 2003-0767.
- Krawczyk J., Ligęza P., Poleszczyk E., Skotniczny P., 2011. *Advanced Hot-Wire Anemometric Measurement Systems in Investigation of the Air Flow Velocity Fields in Mine Headings*. Archives of Mining Sciences **56**, 4.
- Skotniczny P., 2015. *Analiza turbulentnej strugi powietrza w pobliżu ociosów wyrobiska górniczego w aspekcie poprawności rozmieszczenia anemometrów stacjonarnych w przekroju pomiarowym*. Przegląd Górniczy **11**.